ISSN 0915-633X

NATIONAL INSTITUTE FOR FUSION SCIENCE

Topological Structure of Magnetic Flux Lines Generated by Thermal Convection in a Rotating Spherical Shell

H. Kitauchi

(Received - Nov. 20, 1997)

NIFS-523 Dec. 1997

RESEARCH REPORT
NIFS Series

NAGOYA, JAPAN

Topological Structure of Magnetic Flux Lines Generated by Thermal Convection in a Rotating Spherical Shell

Hideaki KITAUCHI

Theory and Computer Simulation Center, National Institute for Fusion Science, Toki 509-52

(Received November 11, 1997)

Topological structure and reconnection of magnetic flux lines are investigated by analyzing the numerical solution of the Boussinesq magneto-hydrodynamic equations in a rotating spherical shell. Five pairs of Taylor-Proudman vortex columns are generated and drift westward steadily. Magnetic field is intensified around the tops of these vortex columns. Magnetic flux lines connect east-west adjacent domains of intense magnetic field, which migrate eastward relative to the vortex columns. We describe the variation of topology of magnetic flux lines associated with this eastward migration.

KEYWORDS: Boussinesq MHD dynamo, thermal convection, rotating spherical shell, reconnection of magnetic flux lines

§1. Introduction

The problem of a magneto-hydrodynamic (MHD) dynamo driven by thermal convection in a rotating spherical shell has been investigated not only for the physical importance, but also for understanding the essential mechanisms of the generation of magnetic field in celestial bodies such as the geodynamo.[1)] A recent rapid development of computer science has enabled us to solve a set of MHD equations numerically.[2–7)]

In a previous paper[7)] we studied an intensification mechanism of magnetic flux density by comparing the structures of the velocity and the magnetic fields near an onset of dynamo action, in which five pairs of cyclonic (i.e. rotating in the same sense as the spherical shell) and anti-cyclonic vortex columns drift westward steadily. The velocity field is symmetric with respect to the equatorial plane and is five-fold symmetric around the rotation axis, whereas the magnetic field is anti-symmetric and is not five-fold symmetric.[8)] This may be attributed to the fact that the asymmetric mode is linearly more unstable than the symmetric one.[9)] The intense magnetic field is always confined in three distinct domains; namely, around the tops of cyclones and their western neighbor anti-cyclones, inside the anti-cyclones, and between cyclones and their western neighbor anti-cyclones. The magnetic field is intensified by concentrate-and-stretch of the magnetic flux lines around sinks in the outer boundary layer, on the equatorial plane and in the inner boundary layer. The domains of intense magnetic field migrate eastward relative to the vortex columns at a speed of much slower than the westward drift of the vortex columns. The magnetic dipole moment oscillates periodically.

In this paper we investigate the topological structure of the intense magnetic flux lines and its temporal evolution in the above magnetic field. In §2 we discuss the possible types of connections of the magnetic flux lines which pass the domains of intense magnetic field. We describe the topology and the reconnection process of the intense magnetic flux lines in §3, and the temporal evolution of the magnetic flux lines outside the outer sphere in §4. Section 5 is devoted to our concluding remarks.

§2. Topology of Magnetic Flux Lines

Before examining the numerical solution of the magnetic field, we consider here the possible topological structures of the intense magnetic flux lines. As stated in the introduction, the present magnetic field is anti-symmetric with respect to the equatorial plane. Among the three domains of intense magnetic field, the magnetic flux density is intensified most strongly around the tops of cyclones and their western neighbor anti-cyclones. There are five of such domains around the rotation axis in each hemisphere, which are illustrated by shaded circles in Fig. 1.

There are at least two possible types of connections of the magnetic flux lines which pass adjacent domains of intense magnetic field, i.e. either the north-south symmetric domains (Fig. 1 (a)) or the east-west adjacent ones (Fig. 1 (b)). Here, thick lines with arrows represent the magnetic flux lines. The magnetic field can be intensified around all of the five domains in the former case, whereas it can not be intensified at least around one of the five in the latter because there is no partner to be connected with this particular one. This latter topological structure of the magnetic flux lines results in an asymmetry of the magnetic field around the rotation axis. As will be described in the next section, the asymmetric case is realized in our numerical magnetic field.

§3. Temporal Evolution of Magnetic Flux Lines

The magnetic field we consider here is driven by the thermal convection of an electrically conducting fluid and confined between two concentric spheres which are rotating with common constant angular velocity in the gravity field pointed to the center. The temperature on each sphere is kept uniform and constant at all the time. It is hotter on the inner sphere than on the outer. The equations of the velocity, the magnetic and the temperature fields under the Boussinesq and the MHD approximations are solved numerically by the pseudo-spectral method described in ref. 6.

The periodic variation of the magnetic dipole moment was described in a previous paper.[7] In Fig. 2 we plot the time-series of the axial component m_z of the magnetic dipole moment over a single period of the oscillation, $481 \leq t \leq 513$. The temporal evolution of the magnetic field during this period is drawn in Fig. 3, which is viewed (a) from the North Pole and (b) from a direction slightly above the equatorial plane. The isosurfaces of the magnitude of magnetic flux density $\boldsymbol{b}$ and vorticity $\boldsymbol{\omega}$ are respectively drawn by yellow and gray at times denoted by solid circles in Fig. 2 in a frame rotating with the vortex columns (hereafter called the steady-flow frame). The points of local maxima of $|\boldsymbol{b}|$ in the domains around the tops of the vortex columns are plotted by red and black. These points are located above the cyclones and are symmetric with respect to the equatorial plane. The red ones belong to a particular cyclone (located at the top in Fig. 3 (a)). A green line represents the magnetic flux line drawn from a red point in the Northern Hemisphere, which also passes the corresponding one in the Southern Hemisphere. Dark (or light) green implies that the magnetic flux lines are inside (or outside) the outer sphere. An arrow denotes the direction of $\boldsymbol{b}$. All the magnetic flux lines are closed and anti-symmetric with respect to the equatorial plane. It is interesting to observe that the magnetic flux line connects the east-west neighboring local maxima of $|\boldsymbol{b}|$, namely, the connection of the magnetic flux lines shown in Fig. 1 (b) is actually realized. The magnetic field is not five-fold symmetric around the rotation axis.

The structures of the magnetic field at (i), (v) and (vi) are identical but their locations are shifted in the longitudinal direction by angle $\frac{2}{5}\pi$ or $\frac{4}{5}\pi$ with each other (compare the yellow isosurfaces in Fig. 3 (a)). Let us assign A, B and C to the corresponding points in the congruent domains of intense magnetic field at (i), (v) and (vi), respectively. Then we notice that $\boldsymbol{b}$ at A, B and C changes the direction in succession. We describe below the variation of the magnetic flux lines during this magnetic field reversal.

A magnetic flux line which comes out of the red point at (i)-(iii) passes near the western local maximum, while that at (iv)-(vi) passes near the eastern local maximum. The reconnection of this magnetic flux line takes place near the poles at some time between (iii) and (iv). The magnetic flux line gradually bends toward the North Pole before the reconnection ((i)-(iii)), and leaves away from the pole after the reconnection ((iv)-(vi)). The same process repeats between (v) and (vi).

§4. Reconnection of Magnetic Flux Lines outside the Sphere

In this section we consider the variation of topological structure of the intense magnetic flux lines outside the outer sphere. In Fig. 4 we plot $|\boldsymbol{b}|$ on the outer sphere by contour lines in the steady-flow frame at every four time unit in the period $481 \leq t \leq 497$ (cf. Fig. 2). The local maxima of $|\boldsymbol{b}|$ are denoted by red. They are viewed from a direction slightly inclined from the North Pole. The intense magnetic field is distributed asymmetrically around the rotation axis. The magnetic flux lines which pass the local maxima are drawn by green lines. where the intensity is represented by the darkness and the direction by arrows. The magnetic flux lines connect the east-west adjacent regions of intense magnetic field or the north-south symmetric ones. Their topological structures at (i) and (v) are identical within a rotation of angle $\frac{2}{5}\pi$ in the longitudinal direction, but the directions of the corresponding magnetic flux lines are reversed. In the following we describe the reconnection process of the magnetic flux lines during this complete reversal of magnetic field.

Let us start with (i), where five local maxima (denoted by integers 1-5) of $|\boldsymbol{b}|$ exist in the higher latitude. The corresponding points at (v) are assigned by integers $1'$-$5'$. The magnetic flux line of Pt. 1 which connects with the western neighbor Pt. 2 at (i) moves to the north and reconnects with the eastern neighbor Pt. 5 after (iii) and becomes a line of Pt. $2'$ at (v), during which $|\boldsymbol{b}|$ is decreasing at Pt. 2 and increasing at Pt. 5. The magnetic flux line of Pt. 2 which connects with the eastern neighbor Pt. 1 at (i) moves to the south, disappears once at (iv), then shows up again as Pt. $3'$ at (v). In this period $|\boldsymbol{b}|$ at Pt. 2 weakens at (i)-(iii), disappears at (iv), but again appears at (v). The magnetic flux line of Pt. 3 which is pointed to the west at (i) extends further and further toward the western neighbor Pt. 4 and becomes a line of Pt. $4'$ at (v), during which $|\boldsymbol{b}|$ at Pt. 4 is increasing. The magnetic flux lines of Pts. 4 and 5 do not change the connections with the western neighbor in this period and become lines of Pts. $5'$ and $1'$, respectively.

In the lower latitude there are three local maxima of $|\boldsymbol{b}|$ on each hemisphere at (i). We assign letters A, B and C to the magnetic flux lines which come out of them in the Northern Hemisphere. They are symmetric with respect to the equatorial plane. The corresponding magnetic flux lines at (v) are denoted by A$'$, B$'$ and C$'$. Lines A and B connect the east-west adjacent regions of intense magnetic field, whereas line C connects the north-south symmetric ones. Line A just expands out in this period and finally becomes line B$'$. Line B changes from the east-west to the north-south connections between (ii) and (iii), and becomes line C$'$ at (v), while $|\boldsymbol{b}|$ around the foot of C and B decreases and increases, respectively. The magnetic field at the foot of C weakens and line C disappears after (iv). A new magnetic flux line appears at the other side of C after (iii), and grows to line A$'$ at (v).

§5. Concluding Remarks

We have examined the topological structure of the intense magnetic flux lines generated by thermal convection of an electrically conducting fluid in a rotating spherical shell. The magnetic flux lines connect the east-west adjacent domains of intense magnetic field around the tops of vortex columns, as is shown schematically in Fig. 1 (b). Because there are five of such domains in each hemisphere, this topology of the magnetic flux lines brings about an asymmetry of the magnetic field around the rotation axis. The magnetic field is reversed periodically in time. The temporal variation of the magnetic field during this reversal has been described in detail by the reconnection, the annihilation and the creation of the magnetic flux lines. Finally, we would like to stress that the description of the magnetic field in terms of the magnetic flux lines together with the isosurface representation is indispensable for understanding the complex three dimensional structure and the temporal evolution.

Acknowledgments

The problem of an MHD dynamo in a rotating spherical shell was first suggested to the author by Prof. S. Kida. The author would like to express cordial gratitude to Prof. S. Kida for his continual encouragement during this study, invaluable discussions as well as providing him the opportunity to work at the Theory and Computer Simulation Center, National Institute for Fusion Science. The author also would like to express hearty gratitude to Dr. K. Araki for his help in an improvement of the numerical code.

References

1) R. T. Merrill, M. W. McElhinny, and P. L. McFadden: *The Magnetic Field of the Earth, Paleomagnetism, the Core, and the Deep Mantle* , (Academic Press, San Diego, 1996).
2) A. Kageyama and T. Sato: Phys Plasmas **4** (1997) 1569
3) A. Kageyama and T. Sato: Phys. Rev. E **55** (1997) 4617.
4) G. A. Glatzmaier and P. H. Roberts: Phys. Earth Planet. Inter. **91** (1995) 63.
5) G. A. Glatzmaier and P. H. Roberts: Nature **377** (1995) 203.
6) S. Kida, K. Araki, and H. Kitauchi: J. Phys Soc. Japan **66** (1997) 2194.
7) H Kitauchi and S. Kida: Phys. Fluids (in press)
8) H. Kitauchi, K. Araki, and S. Kida: Nonlinearity **10** (1997) 885.
9) K. Araki, H. Kitauchi, and S. Kida: Kokyuroku RIMS **970** (1996) 54 (in Japanese).

Figure Captions

Fig. 1. Two possible topological structures of intense magnetic flux lines (thick lines) which connect (a) the north-south symmetric domains (shaded circles) of intense magnetic field and (b) the east-west adjacent domains. Arrows denote the directions of the magnetic field.

Fig. 2. A periodic oscillation of the axial component m_z of the magnetic dipole moment. Solid circles denote the times of Fig. 3 (i-vi).

Fig. 3. The temporal variation of structures of the magnetic field $\boldsymbol{b}$ and the vorticity field ω, which is viewed (a) from the North Pole and (b) from a direction slightly above the equatorial plane. The isosurfaces of $|\boldsymbol{b}| = 2$ and $|\omega| = 52$ are respectively drawn by yellow and gray at times denoted by solid circles in Fig. 2 in the steady-flow frame. The points of local maxima of $|\boldsymbol{b}|$ are plotted by red and black. A green line represents the magnetic flux line drawn from a red point in the Northern Hemisphere. Dark (or light) green implies that the magnetic flux lines are inside (or outside) the outer sphere. Arrow denotes the direction of $\boldsymbol{b}$.

Fig. 4. The temporal variation of structure of the magnetic field outside the outer sphere. The magnitude of magnetic flux density $|\boldsymbol{b}|$ on the outer sphere is represented by contour lines at the levels of 0.2, 0.4, 0.6, 0.8, 1 in the steady-flow frame at every four time unit in the period $481 \leq t \leq 497$. The regions of local maxima of $|\boldsymbol{b}|$ are denoted by red. They are viewed from a direction slightly inclined from the North Pole. The magnetic flux lines which pass the intense local maxima of $|\boldsymbol{b}|$ on the sphere are drawn by green lines where the intensity is represented by the darkness and the direction by arrows.

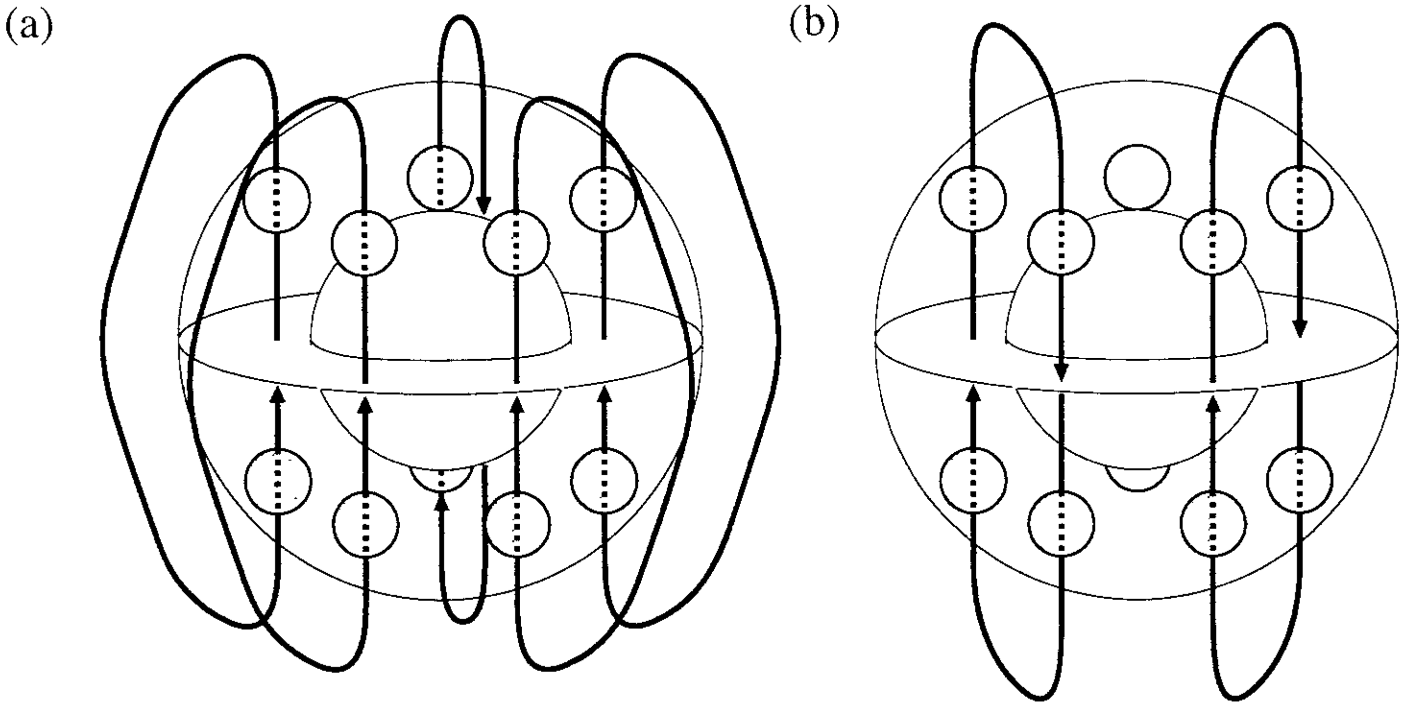

Fig. 1:
H. Kitauchi

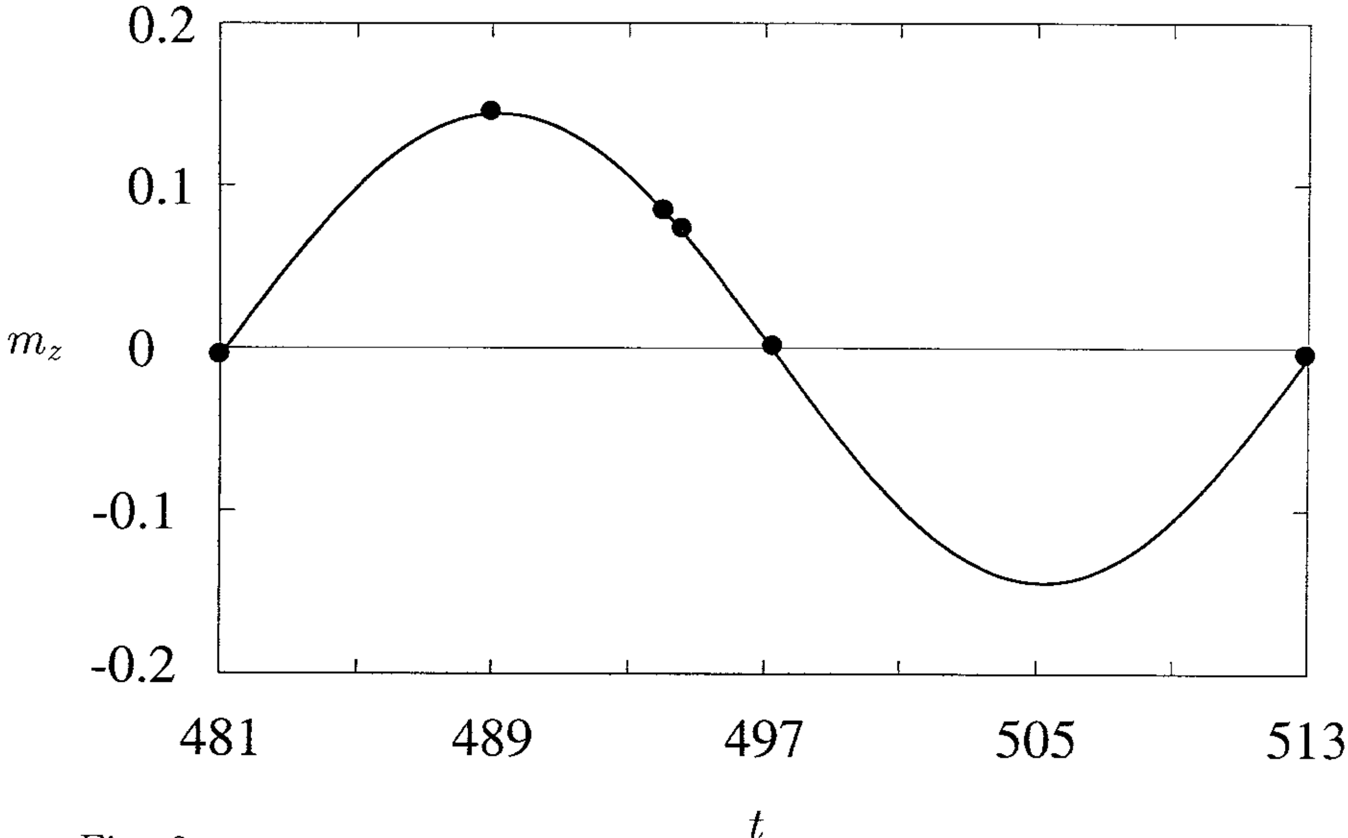

Fig. 2:

H. Kitauchi

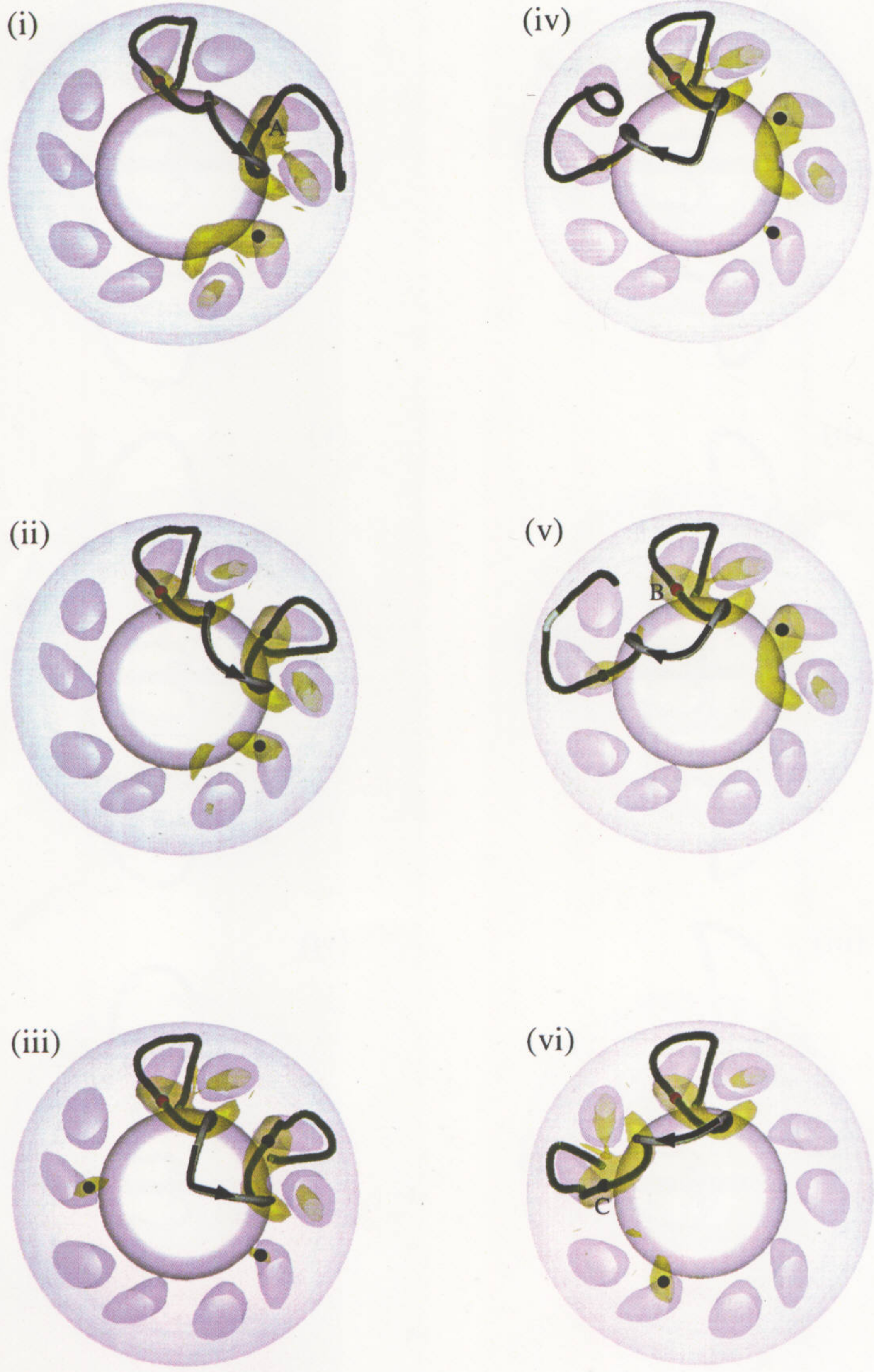

Fig. 3 (a):
H. Kitauchi

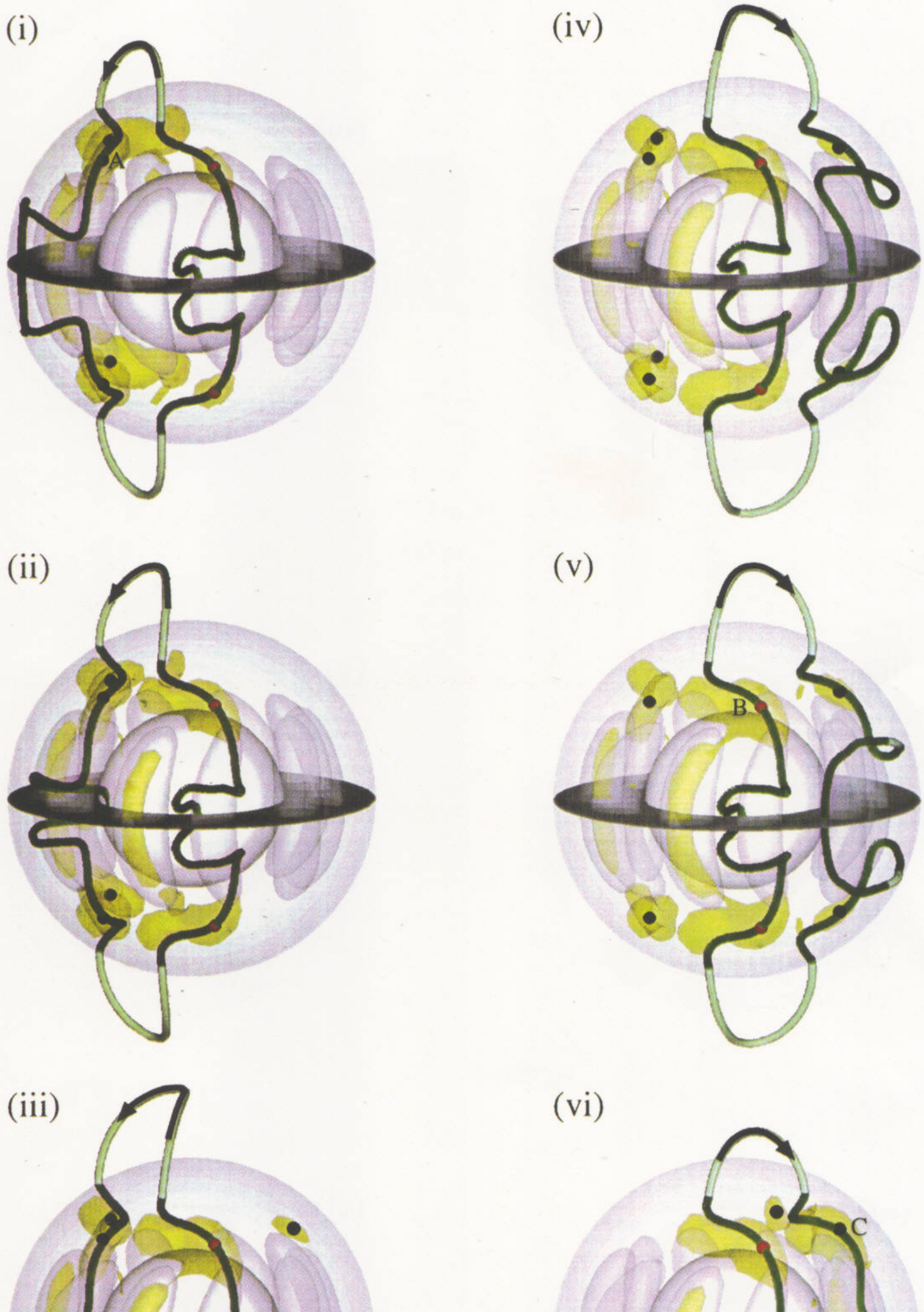

Fig. 3 (b):
H. Kitauchi

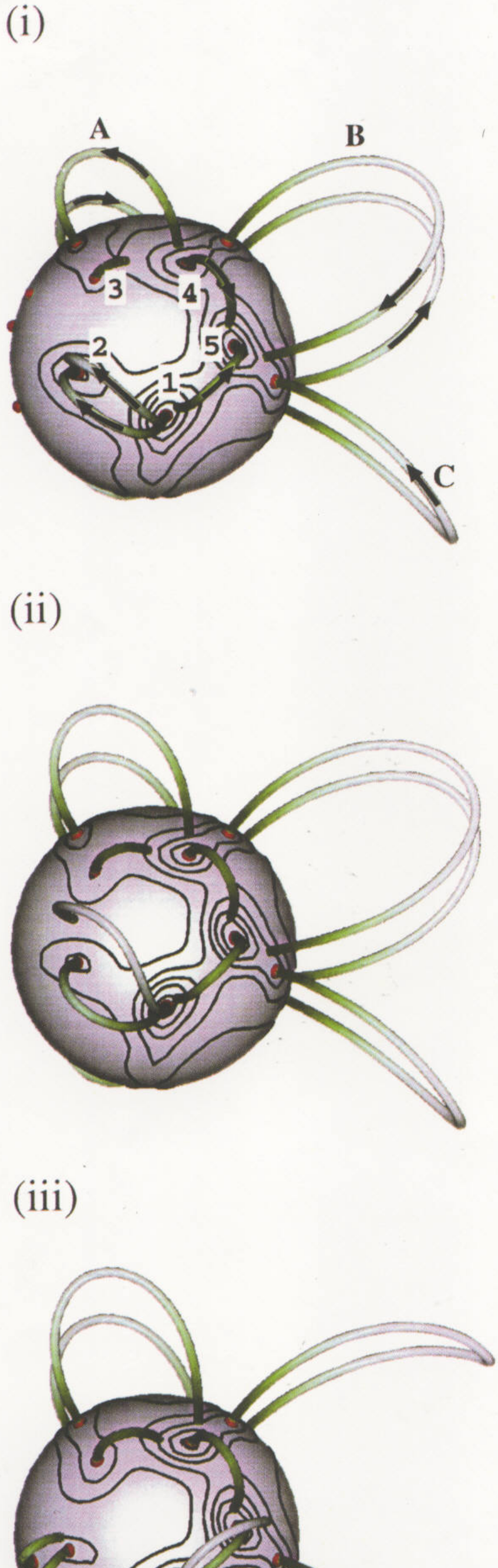

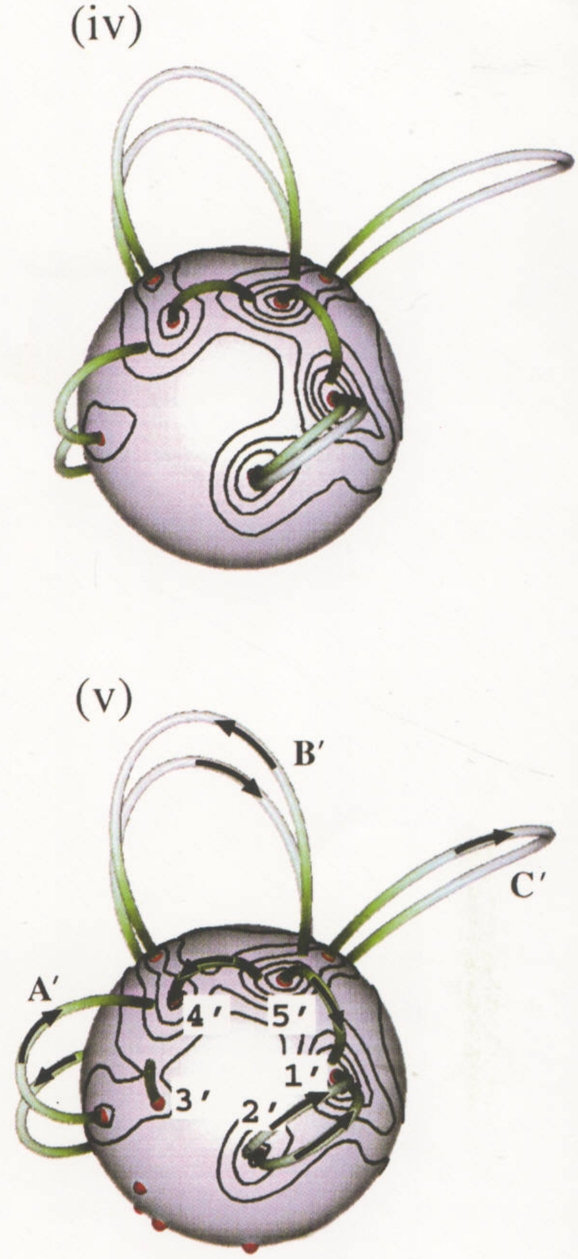

Fig. 4:
H. Kitauchi

Recent Issues of NIFS Series

NIFS-475 A. Fujisawa, H. Iguchi, S. Lee and Y. Hamada,
Consideration of Fluctuation in Secondary Beam Intensity of Heavy Ion Beam Prove Measurements; Jan. 1997

NIFS-476 Y. Takeiri, M. Osakabe, Y. Oka, K. Tsumori, O. Kaneko, T. Takanashi, E. Asano, T. Kawamoto, R. Akiyama and T. Kuroda,
Long-pulse Operation of a Cesium-Seeded High-Current Large Negative Ion Source; Jan. 1997

NIFS-477 H. Kuramoto, K. Toi, N. Haraki, K. Sato, J. Xu, A. Ejiri, K. Narihara, T. Seki, S. Ohdachi, K. Adati, R. Akiyama, Y. Hamada, S. Hirokura, K. Kawahata and M. Kojima,
Study of Toroidal Current Penetration during Current Ramp in JIPP T-IIU with Fast Response Zeeman Polarimeter; Jan., 1997

NIFS-478 H. Sugama and W. Horton,
Neoclassical Electron and Ion Transport in Toroidally Rotating Plasmas; Jan. 1997

NIFS-479 V.L. Vdovin and I.V. Kamenskij,
3D Electromagnetic Theory of ICRF Multi Port Multi Loop Antenna; Jan. 1997

NIFS-480 W.X. Wang, M. Okamoto, N. Nakajima, S Murakami and N. Ohyabu,
Cooling Effect of Secondary Electrons in the High Temperature Divertor Operation; Feb. 1997

NIFS-481 K. Itoh. S.-I. Itoh, H. Soltwisch and H.R. Koslowski,
Generation of Toroidal Current Sheet at Sawtooth Crash; Feb. 1997

NIFS-482 K. Ichiguchi,
Collisionality Dependence of Mercier Stability in LHD Equilibria with Bootstrap Currents; Feb. 1997

NIFS-483 S. Fujiwara and T. Sato,
Molecular Dynamics Simulations of Structural Formation of a Single Polymer Chain: Bond-orientational Order and Conformational Defects; Feb. 1997

NIFS-484 T. Ohkawa,
Reduction of Turbulence by Sheared Toroidal Flow on a Flux Surface; Feb. 1997

NIFS-485 K. Narihara, K. Toi, Y. Hamada, K. Yamauchi, K. Adachi, I. Yamada, K. N. Sato, K. Kawahata, A. Nishizawa, S. Ohdachi, K. Sato, T. Seki, T. Watari, J. Xu, A. Ejiri, S. Hirokura, K. Ida, Y. Kawasumi, M. Kojima, H. Sakakita, T. Ido, K. Kitachi, J. Koog and H. Kuramoto,
Observation of Dusts by Laser Scattering Method in theJIPPT-IIU Tokamak

Mar. 1997

NIFS-486 S. Bazdenkov, T. Sato and The Complexity Simulation Group,
Topological Transformations in Isolated Straight Magnetic Flux Tube; Mar. 1997

NIFS-487 M. Okamoto,
Configuration Studies of LHD Plasmas; Mar. 1997

NIFS-488 A. Fujisawa, H. Iguchi, H. Sanuki, K. Itoh, S. Lee, Y. Hamada, S. Kubo, H. Idei, R. Akiyama, K. Tanaka, T. Minami, K. Ida, S. Nishimura, S. Morita, M. Kojima, S. Hidekuma, S.-I. Itoh, C. Takahashi, N. Inoue, H. Suzuki, S. Okamura and K. Matsuoka,
Dynamic Behavior of Potential in the Plasma Core of the CHS Heliotron/Torsatron; Apr. 1997

NIFS-489 T. Ohkawa,
Pfirsch - Schlüter Diffusion with Anisotropic and Nonuniform Superthermal Ion Pressure; Apr. 1997

NIFS-490 S. Ishiguro and The Complexity Simulation Group,
Formation of Wave-front Pattern Accompanied by Current-driven Electrostatic Ion-cyclotron Instabilities; Apr. 1997

NIFS-491 A. Ejiri, K. Shinohara and K. Kawahata,
An Algorithm to Remove Fringe Jumps and its Application to Microwave Reflectometry; Apr. 1997

NIFS-492 K. Ichiguchi, N. Nakajima, M. Okamoto,
Bootstrap Current in the Large Helical Device with Unbalanced Helical Coil Currents; Apr. 1997

NIFS-493 S. Ishiguro, T. Sato, H. Takamaru and The Complexity Simulation Group,
V-shaped dc Potential Structure Caused by Current-driven Electrostatic Ion-cyclotron Instability; May 1997

NIFS-494 K. Nishimura, R. Horiuchi, T. Sato,
Tilt Stabilization by Energetic Ions Crossing Magnetic Separatrix in Field-Reversed Configuration; June 1997

NIFS-495 T. -H. Watanabe and T. Sato,
Magnetohydrodynamic Approach to the Feedback Instability; July 1997

NIFS-496 K. Itoh, T. Ohkawa, S. -I.Itoh, M. Yagi and A. Fukuyama
Suppression of Plasma Turbulence by Asymmetric Superthermal Ions; July 1997

NIFS-497 T. Takahashi, Y. Tomita, H. Momota and Nikita V. Shabrov,
Collisionless Pitch Angle Scattering of Plasma Ions at the Edge Region of an FRC; July 1997

NIFS-498 M. Tanaka, A.Yu Grosberg, V.S. Pande and T. Tanaka,
Molecular Dynamics and Structure Organization in Strongly-Coupled Chain of Charged Particles; July 1997

NIFS-499 S. Goto and S. Kida,
Direct-interaction Approximation and Reynolds-number Reversed Expansion for a Dynamical System; July 1997

NIFS-500 K. Tsuzuki, N. Inoue, A. Sagara, N. Noda, O. Motojima, T. Mochizuki, T. Hino and T. Yamashina,
Dynamic Behavior of Hydrogen Atoms with a Boronized Wall; July 1997

NIFS-501 I. Viniar and S. Sudo,
Multibarrel Repetitive Injector with a Porous Pellet Formation Unit; July 1997

NIFS-502 V. Vdovin, T. Watari and A. Fukuyama,
An Option of ICRF Ion Heating Scenario in Large Helical Device; July 1997

NIFS-503 E. Segre and S. Kida,
Late States of Incompressible 2D Decaying Vorticity Fields; Aug. 1997

NIFS-504 S. Fujiwara and T. Sato,
Molecular Dynamics Simulation of Structural Formation of Short Polymer Chains; Aug. 1997

NIFS-505 S. Bazdenkov and T. Sato
Low-Dimensional Model of Resistive Interchange Convection in Magnetized Plasmas; Sep. 1997

NIFS-506 H. Kitauchi and S. Kida,
Intensification of Magnetic Field by Concentrate-and-Stretch of Magnetic Flux Lines; Sep. 1997

NIFS-507 R.L. Dewar,
Reduced form of MHD Lagrangian for Ballooning Modes; Sep. 1997

NIFS-508 Y.-N. Nejoh,
Dynamics of the Dust Charging on Electrostatic Waves in a Dusty Plasma with Trapped Electrons; Sep.1997

NIFS-509 E. Matsunaga, T.Yabe and M. Tajima,
Baroclinic Vortex Generation by a Comet Shoemaker-Levy 9 Impact; Sep. 1997

NIFS-510 C.C. Hegna and N. Nakajima,
On the Stability of Mercier and Ballooning Modes in Stellarator Configurations; Oct. 1997

NIFS-511 K. Orito and T. Hatori,
Rotation and Oscillation of Nonlinear Dipole Vortex in the Drift-Unstable Plasma; Oct. 1997

NIFS-512 J. Uramoto,
Clear Detection of Negative Pionlike Particles from H_2 Gas Discharge in Magnetic Field; Oct. 1997

NIFS-513 T. Shimozuma, M. Sato, Y. Takita, S. Ito, S. Kubo, H. Idei, K. Ohkubo, T. Watari, T.S. Chu, K. Felch, P. Cahalan and C.M. Loring, Jr,
The First Preliminary Experiments on an 84 GHz Gyrotron with a Single-Stage Depressed Collector; Oct. 1997

NIFS-514 T. Shjmozuma, S. Morimoto, M. Sato, Y. Takita, S. Ito, S. Kubo, H. Idei, K. Ohkubo and T. Watari,
A Forced Gas-Cooled Single-Disk Window Using Silicon Nitride Composite for High Power CW Millimeter Waves; Oct. 1997

NIFS-515 K. Akaishi,
On the Solution of the Outgassing Equation for the Pump-down of an Unbaked Vacuum System; Oct. 1997

NIFS-516 *Papers Presented at the 6th H-mode Workshop (Seeon, Germany)*; Oct. 1997

NIFS-517 John L. Johnson,
The Quest for Fusion Energy; Oct. 1997

NIFS-518 J. Chen, N. Nakajima and M. Okamoto,
Shift-and-Inverse Lanczos Algorithm for Ideal MHD Stability Analysis; Nov. 1997

NIFS-519 M. Yokoyama, N. Nakajima and M. Okamoto,
Nonlinear Incompressible Poloidal Viscosity in L=2 Heliotron and Quasi-Symmetric Stellarators; Nov. 1997

NIFS-520 S. Kida and H. Miura,
Identificaiton and Analysis of Vortical Structures; Nov. 1997

NIFS-521 K. Ida, S. Nishimura, T. Minami, K. Tanaka, S. Okamura, M. Osakabe, H. Idei, S. Kubo, C. Takahashi and K. Matsuoka,
High Ion Temperature Mode in CHS Heliotron/torsatron Plasmas; Nov. 1997

NIFS-522 M. Yokoyama, N. Nakajima and M. Okamoto,
Realization and Classification of Symmetric Stellarator Configurations through Plasma Boundary Modulations; Dec. 1997

NIFS-523 H. Kitauchi,
Topological Structure of Magnetic Flux Lines Generated by Thermal Convection in a Rotating Spherical Shell; Dec. 1997